The complex variable meshless local Petrov–Galerkin method of solving two-dimensional potential problems*

Yang Xiu-Li(杨秀丽), Dai Bao-Dong (戴保东)†, and Zhang Wei-Wei(张伟伟)

Department of Engineering Mechanics, Taiyuan University of Science & Technology, Taiyuan 030024, *China*

(Received 28 February 2012; revised manuscript received 22 March 2012)

Based on the complex variable moving least-square (CVMLS) approximation and a local symmetric weak form, the complex variable meshless local Petrov–Galerkin (CVMLPG) method of solving two-dimensional potential problems is presented in this paper. In the present formulation, the trial function of a two-dimensional problem is formed with a one-dimensional basis function. The number of unknown coefficients in the trial function of the CVMLS approximation is less than that in the trial function of the moving least-square (MLS) approximation. The essential boundary conditions are imposed by the penalty method. The main advantage of this approach over the conventional meshless local Petrov–Galerkin (MLPG) method is its computational efficiency. Several numerical examples are presented to illustrate the implementation and performance of the present CVMLPG method.

Keywords: meshless method, complex variable moving least-square method, complex variable meshless local Petrov–Galerkin method, potential problems

PACS: 02.60.–x, 02.70.Pt, 02.70.–c, 46.25.–y **DOI:** 10.1088/1674-1056/21/10/100208

1. Introduction

Most engineering problems and various physical problems may boil down to partial differential equations. The potential problem is one of the most important partial differential equations in engineering mathematics because it is related to gravitational fields, electrostatics fields, steady-state heat conductions, and many other areas.[1] Well-known potential problems include the Laplace or Poisson equations in a given domain with a boundary condition. However, when the boundary conditions or material properties of the discussed models are too complex, their analytical solutions are usually difficult to obtain. Therefore, for many decades, researchers have made considerable efforts to develop efficient numerical methods to solve these problems.

The finite element method (FEM) has been one of the well-established numerical solutions for engineering problems over the past a few decades. However, it also has limitations, the reliance of the FEM on a mesh leads to complications for some kinds of problems, especially extremely large deformation, dynamic fracturing, and explosion problems. In addition, mesh generation can be a very time-consuming and burdensome task especially when a re-meshing is required in the computing process.

Over the past twenty years, meshless or element free methods have been developed as alternative numerical approaches by eliminating disadvantages existing in the FEM. Meshless methods each require only a set of nodes to scatter the problem domain and construct the approximate functions. So meshless methods can be used to solve many engineering problems that cannot be solved by conventional numerical methods based on meshes or elements. In recent years, meshless methods have become important methods in computational mechanics.[2,3] During the last two decades, several meshless methods of seeking approximate solutions of partial differential equations have been proposed, which include the element-free Galerkin (EFG) method,[4,5] the meshless local Petrov–Galerkin (MLPG) method,[6–8] the reproducing kernel particle method (RKPM),[9,10] and the complex variable meshless method.[11,12]

The main difference between the meshless methods is the way the shape function is formulated. The moving least-square (MLS) approximation is an important method to form the shape function in the meshless methods.[13] The advantages of the MLS

*Project supported by the Young Scientists Fund of the National Natural Science Foundation of China (Grant No. 11102125).
†Corresponding author. E-mail: Dai_baodong@126.com
© 2012 Chinese Physical Society and IOP Publishing Ltd

approximation are as follows: (i) the approximation function is continuous and smooth in the entire problem domain; (ii) it is capable of producing an approximation with the desired order of consistency. However, in practical numerical processes, the computational cost of the MLS approximation is quite burdensome, and sometimes this method can form an ill-conditioned system of equations.[14,15]

To overcome the shortcomings of the MLS method, a new approximation technique, a complex variable moving least-square (CVMLS) approximation in which the trial function of a two-dimensional (2D) problem is formed with a one-dimensional (1D) basis function has been developed by Liew *et al.*[16] and Cheng *et al.*[17] In the CVMLS approximation, the number of unknown coefficients is less than that in the trial function of the MLS approximation. Therefore fewer nodes are needed in the meshless method, which are formed from the CVMLS approximation than those from the MLS approximation with no loss of accuracy. Hence, under the same numerical accuracy, the meshless method based on the CVMLS approximation has a greater computational efficiency. The complex variable meshless method was developed on the basis of the CVMLS, and was then applied to 2D elasticity,[18,19] fracture problems,[20] and elastic large deformation problems.[21] Based on the CVMLS approximation and the boundary element-free method, a complex variable boundary element-free method of 2D elastodynamic problems was proposed.[12] On the basis of reproducing kernel particle method, the complex variable reproducing kernel particle method was developed and applied to 2D elasticity and transient heat conduction problems.[22,23] Based on the CVMLS approximation and the finite cover theory, the complex variable meshless manifold method (CVMMM) was presented.[24,25] The CVMLPG approach to solving problems in elasto-statics was developed, using a local symmetric weak form and shape functions from the CVMLS approximation.[26]

In the present paper, the CVMLPG approach to solving 2D potential problems is developed and numerically implemented. In the presented method a local symmetric weak form and shape functions from the CVMLS approximation are used. In the presented formulation, the trial function of a 2D problem is formed with a 1D basis function. The penalty formulation is used to impose the essential boundary conditions in the presented approach. The presented CVMLPG method is promising as it reduces the computational time of the conventional MLPG method. The formulations of the CVMLPG method are given together with some numerical examples to demonstrate the applicability of the present method.

2. Complex variable moving least-square approximation

In the CVMLPG method, CVMLS approximation is employed for the construction of the shape function.

Let $\tilde{u}(z)$ be the function of the field variable defined in the domain Ω. The approximation of $\tilde{u}(z)$ at point z is denoted as $u^h(z)$, and the trial function is

$$\begin{aligned} u^h(z) &= u_1^h(z) + \mathrm{i}u_2^h(z) = \sum_{j=1}^{m} p_j(z)a_j(z) \\ &= \boldsymbol{p}^{\mathrm{T}}(z)\boldsymbol{a}(z), \quad z = x_1 + \mathrm{i}x_2 \in \Omega, \end{aligned} \tag{1}$$

where $p_j(z)$ are monomial basis functions, $a_j(z)$ are the coefficients of the basis functions, and m is the number of terms in the basis.

The local approximation at point z is described as

$$u^h(z,\bar{z}) = \sum_{j=1}^{m} p_j(\bar{z})a_j(z) = \boldsymbol{p}^{\mathrm{T}}(\bar{z})\boldsymbol{a}(z), \tag{2}$$

where $\bar{z}$ is the point in the local domain of z.

To accurately obtain the local approximation of the function $\tilde{u}(z)$, the difference between local approximation $u^h(z)$ and function $\tilde{u}(z)$ must be minimized by a weighted least-square method.

Define the quadratic form as

$$\begin{aligned} J &= \sum_{I=1}^{n} w(z-z_I)\left[u^h(z,z_I) - \tilde{u}(z_I)\right]^2 \\ &= \sum_{I=1}^{n} w(z-z_I)\Big[\sum_{j=1}^{m} p_j(z_I)a_j(z) - \tilde{u}(z_I)\Big]^2, \end{aligned} \tag{3}$$

where z_I $(I = 1, 2, \ldots, n)$ are the nodes with domains of influence which cover the point z and $w(z-z_I)$ is a weight function with a domain of influence.

$$\tilde{u}(z_I) = u_1(z_I) + \mathrm{i}u_2(z_I). \tag{4}$$

Equation (3) can be rewritten in a vector form as

$$J = (\boldsymbol{P}\boldsymbol{a} - \tilde{\boldsymbol{u}})^{\mathrm{T}}\boldsymbol{W}(z)(\boldsymbol{P}\boldsymbol{a} - \tilde{\boldsymbol{u}}), \tag{5}$$

where $\tilde{\boldsymbol{u}}$ is the vector that collects the nodal parameters of the field variables for all of the nodes in the

support domain, and it is expressed as

$$\tilde{\boldsymbol{u}} = (\tilde{u}(z_1), \tilde{u}(z_2), \ldots, \tilde{u}(z_n))^{\mathrm{T}} = \boldsymbol{Q}\boldsymbol{u}, \tag{6}$$

with

$$\boldsymbol{Q} = \begin{pmatrix} 1 & \mathrm{i} & 0 & 0 & 0 & 0 & \cdots & 0 & 0 \\ 0 & 0 & 1 & \mathrm{i} & 0 & 0 & \cdots & 0 & 0 \\ 0 & 0 & 0 & 0 & 1 & \mathrm{i} & \cdots & 0 & 0 \\ \vdots & \vdots & \vdots & \vdots & \vdots & \vdots & \ddots & \vdots & \vdots \\ 0 & 0 & 0 & 0 & 0 & 0 & \cdots & 1 & \mathrm{i} \end{pmatrix}_{n\times 2n}, \tag{7}$$

$$\boldsymbol{u} = (u_1(z_1), u_2(z_1), u_1(z_2), u_2(z_2), \cdots, u_1(z_n), u_2(z_n))^{\mathrm{T}}, \tag{8}$$

$$\boldsymbol{P} = \begin{pmatrix} p_1(z_1) & p_2(z_1) & \cdots & p_m(z_1) \\ p_1(z_2) & p_2(z_2) & \cdots & p_m(z_2) \\ \vdots & \vdots & \ddots & \vdots \\ p_1(z_n) & p_2(z_n) & \cdots & p_m(z_n) \end{pmatrix}_{n\times m}, \tag{9}$$

$$\boldsymbol{W}(z) = \begin{pmatrix} w(z-z_1) & 0 & \cdots & 0 \\ 0 & w(z-z_2) & \cdots & 0 \\ \vdots & \vdots & \ddots & \vdots \\ 0 & 0 & \cdots & w(z-z_n) \end{pmatrix}_{n\times n}. \tag{10}$$

The minimization condition requires

$$\frac{\partial J}{\partial \boldsymbol{a}} = \boldsymbol{A}(z)\boldsymbol{a}(z) - \boldsymbol{B}(z)\tilde{\boldsymbol{u}} = 0, \tag{11}$$

which results in the equation system

$$\boldsymbol{A}(z)\boldsymbol{a}(z) = \boldsymbol{B}(z)\tilde{\boldsymbol{u}}, \tag{12}$$

where matrices $\boldsymbol{A}(z)$ and $\boldsymbol{B}(z)$ are

$$\boldsymbol{A}(z) = \boldsymbol{P}^{\mathrm{T}}\boldsymbol{W}(z)\boldsymbol{P}, \tag{13}$$

$$\boldsymbol{B}(z) = \boldsymbol{P}^{\mathrm{T}}\boldsymbol{W}(z). \tag{14}$$

From Eq. (12), we can obtain

$$\boldsymbol{a}(z) = \boldsymbol{A}^{-1}(z)\boldsymbol{B}(z)\tilde{\boldsymbol{u}}. \tag{15}$$

The expression of the local approximation $u^h(z)$ is thus

$$u^h(z) = \boldsymbol{\Phi}(z)\tilde{\boldsymbol{u}} = \sum_{I=1}^{n} \Phi_I(z)\tilde{u}(z_I) = u_1^h(z) + \mathrm{i}u_2^h(z). \tag{16}$$

Therefore we have

$$u_1^h(z) = \mathrm{Re}[\boldsymbol{\Phi}(z)\tilde{\boldsymbol{u}}] = \mathrm{Re}\Big[\sum_{I=1}^{n} \Phi_I(z)\tilde{u}(z_I)\Big], \tag{17}$$

$$u_2^h(z) = \mathrm{Im}[\boldsymbol{\Phi}(z)\tilde{\boldsymbol{u}}] = \mathrm{Im}\Big[\sum_{I=1}^{n} \Phi_I(z)\tilde{u}(z_I)\Big], \tag{18}$$

where $\boldsymbol{\Phi}(z)$ is defined as the shape function of the CVMLS, and

$$\boldsymbol{\Phi}(z) = (\phi_1(z), \phi_2(z), \ldots, \phi_n(z)) = \boldsymbol{p}^{\mathrm{T}}(z)\boldsymbol{A}^{-1}(z)\boldsymbol{B}(z). \tag{19}$$

This is the CVMLS approximation.

3. CVMLPG method of solving 2D potential problems

Consider a Poisson's equation for a problem governing the potential u in a 2D domain Ω bounded by contour Γ ($\Gamma = \Gamma_u \cup \Gamma_t$),

$$\nabla^2 u = p(\boldsymbol{x}), \ \text{in} \ \Omega, \tag{20}$$

$$u = \bar{u}, \quad \boldsymbol{x} \in \Gamma_u, \tag{21}$$

$$q = \frac{\partial u}{\partial n} = \bar{q}, \quad \boldsymbol{x} \in \Gamma_t, \tag{22}$$

where $p(\boldsymbol{x})$ is a given source function, u is an unknown function, and n is the unit outward normal to the boundary Γ, $\bar{u}$ and $\bar{q}$ are the prescribed values of the function u and its normal derivative over the boundary Γ.

The use of the CVMLS approximation produces shape functions that do not possess the Kronecker delta function property. This implies that essential boundary conditions cannot be imposed directly. In this paper, we impose essential boundary conditions by using penalty factors. Now, consider the problem stated in Eqs. (20)–(22). We introduce a penalty factor α to impose the essential boundary conditions.

Using the local weighted residual method, the generalized local weak form of Eq. (20) can be obtained as

$$\int_{\Omega_{\mathrm{q}}} v_I(\nabla^2 u - p(z))\,\mathrm{d}\Omega - \alpha \int_{\Gamma_{\mathrm{qu}}} v_I(u-\bar{u})\,\mathrm{d}\Gamma = 0, \tag{23}$$

where v_I is the test function with compact support of node z_I, Ω_{q} denotes the local domain of z_I, Γ_{qu} denotes the essential boundaries, α is a penalty parameter (factor) which is assigned to the constant of a large positive number.

By the subsection integration and the divergence theorem, Eq. (23) can be written as

$$\int_{\Gamma_{\mathrm{q}}} v_I n_i u_{,i}\,\mathrm{d}\Gamma - \int_{\Omega_{\mathrm{q}}} (v_{I,i}u_{,i} + v_I p)\,\mathrm{d}\Omega - \alpha \int_{\Gamma_{\mathrm{qu}}} v_I(u-\bar{u})\,\mathrm{d}\Gamma = 0, \quad (i = 1, 2). \tag{24}$$

The boundary Γ_{q} of the integral sub-domain Ω_{q}

can be separated as follows:

$$\Gamma_{\rm q} = \Gamma_{\rm qi} \cup \Gamma_{\rm qt} \cup \Gamma_{\rm qu}, \tag{25}$$

where $\Gamma_{\rm qi}$ is part of the internal boundary of $\Omega_{\rm q}$ where no boundary condition is specified, $\Gamma_{\rm qt}$ is the natural boundaries which intersect with $\Omega_{\rm q}$.

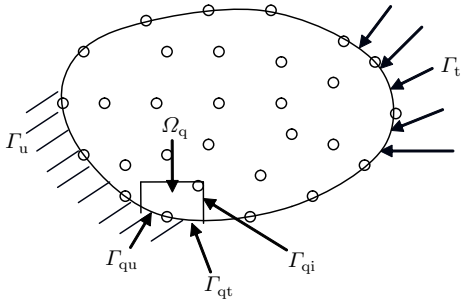


Fig. 1. Boundary conditions of sub-domain.

Equation (24) can also be rewritten as

$$\int_{\Gamma_{\rm qi}} v_I n_i u_{,i} {\rm d}\Gamma + \int_{\Gamma_{\rm qt}} v_I n_i u_{,i} {\rm d}\Gamma + \int_{\Gamma_{\rm qu}} v_I n_i u_{,i} {\rm d}\Gamma - \int_{\Omega_{\rm q}} (v_{I,i} u_{,i} + v_I p) {\rm d}\Omega - \alpha \int_{\Gamma_{\rm qu}} v_I (u - \bar{u}) {\rm d}\Gamma = 0. \tag{26}$$

In order to simplify Eq. (26), weight function v_I is used as a Heaviside step function

$$v_I(z) = \begin{cases} c, & z \in \Omega_{\rm q}, \\ 0, & z \notin \Omega_{\rm q}, \end{cases} \tag{27}$$

where c is an arbitrary constant (c is chosen to be 1 in this paper).

Using the Heaviside step function as the weight function, the local weak form (26) can be rewritten as

$$\int_{\Gamma_{\rm qi}} n_i u_{,i} {\rm d}\Gamma + \int_{\Gamma_{\rm qt}} n_i u_{,i} {\rm d}\Gamma + \int_{\Gamma_{\rm qu}} n_i u_{,i} {\rm d}\Gamma - \int_{\Omega_{\rm q}} p {\rm d}\Omega - \alpha \int_{\Gamma_{\rm qu}} (u - \bar{u}) {\rm d}\Gamma = 0. \tag{28}$$

Substituting the natural boundary conditions into Eq. (28), we have

$$-\int_{\Gamma_{\rm qi}} n_i u_{,i} {\rm d}\Gamma - \int_{\Gamma_{\rm qu}} n_i u_{,i} {\rm d}\Gamma + \alpha \int_{\Gamma_{\rm qu}} u {\rm d}\Gamma = -\int_{\Omega_{\rm q}} p {\rm d}\Omega + \alpha \int_{\Gamma_{\rm qu}} \bar{u} {\rm d}\Gamma + \int_{\Gamma_{\rm qt}} \bar{q} {\rm d}\Gamma. \tag{29}$$

From the CVMLS approximation (16), the potential at an arbitrary point z in the domain can be expressed as follows:

$$\begin{aligned} u(z) &= {\rm Re}[\boldsymbol{\Phi}(z)\boldsymbol{u}] = \sum_{I=1}^{n} {\rm Re}[\Phi_I(z)] u(z_I) \\ &= \tilde{\boldsymbol{\Phi}}(z)\boldsymbol{u}, \end{aligned} \tag{30}$$

where

$$\tilde{\boldsymbol{\Phi}}(z) = (\tilde{\Phi}_1(z), \tilde{\Phi}_2(z), \ldots, \tilde{\Phi}_n(z)), \tag{31}$$

$$\tilde{\Phi}_I(z) = {\rm Re}[\Phi_I(z)], \tag{32}$$

$$\boldsymbol{u} = (u(z_1), u(z_2), \ldots, u(z_n))^{\rm T}. \tag{33}$$

Substituting Eq. (30) into Eq. (29), the resulting system equation is obtained as follows:

$$\Big[-\int_{\Gamma_{\rm qi}} \boldsymbol{n}\boldsymbol{B} {\rm d}\Gamma - \int_{\Gamma_{\rm qu}} \boldsymbol{n}\boldsymbol{B} {\rm d}\Gamma + \alpha \int_{\Gamma_{\rm qu}} \tilde{\boldsymbol{\Phi}} {\rm d}\Gamma\Big]\boldsymbol{u} = -\int_{\Omega_{\rm q}} \boldsymbol{p} {\rm d}\Omega + \alpha \int_{\Gamma_{\rm qu}} \bar{\boldsymbol{u}} {\rm d}\Gamma + \int_{\Gamma_{\rm qt}} \bar{\boldsymbol{q}} {\rm d}\Gamma, \tag{34}$$

where

$$\boldsymbol{n} = (n_{x1}, n_{x2}), \tag{35}$$

$$\boldsymbol{B}(z) = (\boldsymbol{B}_1(z), \boldsymbol{B}_2(z), \ldots, \boldsymbol{B}_n(z)), \tag{36}$$

$$\boldsymbol{B}_I(z) = \begin{bmatrix} {\rm Re}[\Phi_{I,1}(z)] \\ {\rm Re}[\Phi_{I,2}(z)] \end{bmatrix}. \tag{37}$$

The matrix form of Eq. (34) is rewritten as

$$(\boldsymbol{k}_I + \boldsymbol{k}_I^{\alpha})\boldsymbol{u} = \boldsymbol{f}_I + \boldsymbol{f}_I^{\alpha}, \tag{38}$$

where $\boldsymbol{k}_I$ is the nodal stiffness matrix for the I-th field node and expressed as

$$\boldsymbol{k}_I = -\int_{\Gamma_{\rm qi}} \boldsymbol{n}\boldsymbol{B} {\rm d}\Gamma - \int_{\Gamma_{\rm qu}} \boldsymbol{n}\boldsymbol{B} {\rm d}\Gamma, \tag{39}$$

$$\boldsymbol{k}_I^{\alpha} = \alpha \int_{\Gamma_{\rm qu}} \tilde{\boldsymbol{\Phi}} {\rm d}\Gamma, \tag{40}$$

where $\boldsymbol{f}_I$ is the nodal load vector for the I-th field node and expressed as

$$\boldsymbol{f}_I = -\int_{\Omega_{\rm q}} \boldsymbol{p} {\rm d}\Omega + \int_{\Gamma_{\rm qt}} \bar{\boldsymbol{q}} {\rm d}\Gamma, \tag{41}$$

$$\boldsymbol{f}_I^{\alpha} = \alpha \int_{\Gamma_{\rm qu}} \bar{\boldsymbol{u}} {\rm d}\Gamma. \tag{42}$$

Equation (38) involves one point z. We need as many local domains $\Omega_{\rm q}$ as the number of nodes in the global domain. Using Eq. (38) for all N field nodes in the entire problem domain, we obtain the following discrete system of equations:

$$\boldsymbol{K}\boldsymbol{U} = \boldsymbol{F} \tag{43}$$

Equation (43) is the final equation system of the complex variable meshless local Petrov–Galerkin method.

4. Numerical examples

In this section, numerical examples will be presented to demonstrate the implementation and the applicability of the present CVMLPG for 2D potential problems. The results obtained from these examples are compared with the existing analytical solutions. In our computation, a regular arrangement of nodes is used to numerically calculate the system equation. The linear basis function is used in the present method.

4.1. Mixed problem of a square

The first example considered is a 2D Laplace equation with mixed boundary conditions in a rectangular domain as shown in Fig. 1. The Laplace equation is

$$\nabla^2 u = \frac{\partial^2 u}{\partial x_1^2} + \frac{\partial^2 u}{\partial x_2^2} = 0, \quad x_1 \in [0,5], \quad x_2 \in [0,10].$$

And the prescribed boundary conditions are

$$\begin{aligned} &u(x_1,0) = 0, && 0 < x_1 < 5,\\ &u(0,x_2) = 0, && 0 < x_2 < 10,\\ &u(x_1,10) = 100\sin(\pi x_1/10), && 0 < x_1 < 5,\\ &\frac{\partial u(5,x_2)}{\partial n} = 0, && 0 < x_2 < 10. \end{aligned}$$

The analytical solution of this problem is

$$u(x_1,x_2) = \frac{100\sin(\pi x_1/10)\sinh(\pi x_2/10)}{\sinh(\pi)}.$$

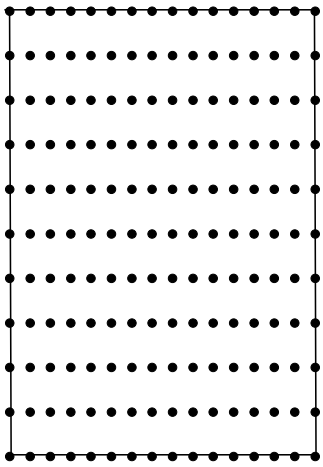


Fig. 2. Node arrangement.

In this analysis, a total of 16×11 nodes are used to represent the problem domain as shown in Fig. 2. The analytical and numerical solutions using the CVMLPG are plotted in Figs. 3 and 4. It is evident that the results from the CVMLPG method accord well with the exact solutions.

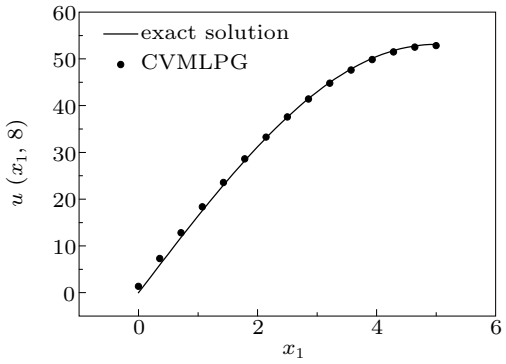


Fig. 3. Exact and numerical solutions of u at $x_2 = 8$.

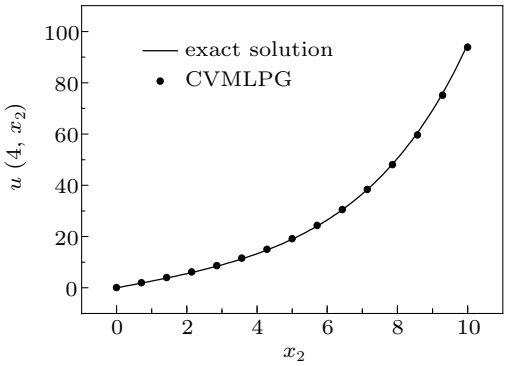


Fig. 4. Exact and numerical solutions of u at $x_1 = 4$.

4.2. Poisson's equation with a Dirichlet problem on a square

The second example considered is a 2D Poisson equation with Dirichlet boundary conditions on the square. The Poisson equation is

$$\nabla^2 u = \frac{\partial^2 u}{\partial x_1^2} + \frac{\partial^2 u}{\partial x_2^2} = x_1 + x_2,\ x_1 \in [0,8],\ x_2 \in [-3,3],$$

with the boundary conditions being

$$\begin{aligned} &u(0,x_2) = -\frac{5}{6}x_2^3, && -3 < x_2 < 3,\\ &u(8,x_2) = -\frac{5}{6}(512 + x_2^3) + 192x_2 + 24x_2^2, && -3 < x_2 < 3,\\ &u(x_1,3) = -\frac{5}{6}(x_1^3 + 27) + 9x_1^2 + 27x_1, && 0 < x_1 < 8,\\ &u(x_1,-3) = -\frac{5}{6}(x_1^3 - 27) - 9x_1^2 + 27x_1, && 0 < x_1 < 8. \end{aligned}$$

The exact solution of this problem is

$$u(x_1,x_2) = -\frac{5}{6}(x_1^3 + x_2^3) + 3x_1^2x_2 + 3x_1x_2^2.$$

Figure 5 shows the distributions of nodes. We employ 40×20 nodes in the domain of the problem. The analytical and numerical results from the

CVMLPG are both shown in Fig. 6. The results from the CVMLPG method well match the analytical solutions.

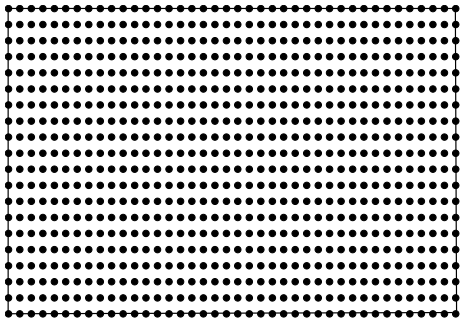


Fig. 5. Node arrangement.

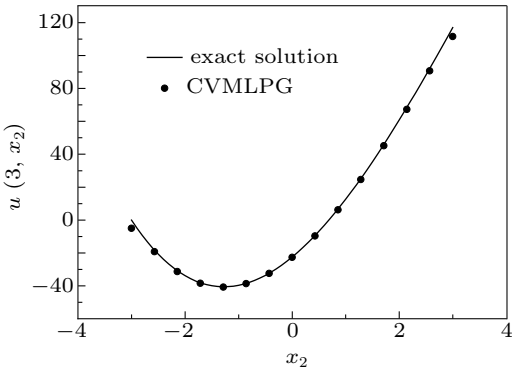


Fig. 6. Exact and numerical solutions of u at $x_1 = 3$.

4.3. Laplace's equation with a Dirichlet problem on a square

A Dirichlet problem is solved in the third example, for which the essential boundary condition is imposed on all sides. The Laplace equation is

$$\nabla^2 u = \frac{\partial^2 u}{\partial x_1^2} + \frac{\partial^2 u}{\partial x_2^2} = 0, \quad x_1 \in [0, 5], \quad x_2 \in [0, 10],$$

with the boundary conditions being

$$u(x_1, 0) = -x_1^3, \quad 0 < x_1 < 5,$$
$$u(0, x_2) = -x_2^3, \quad 0 < x_2 < 10,$$
$$u(x_1, 10) = -x_1^3 + 30x_1^2 + 300x_1 - 1000, \ 0 < x_1 < 5,$$
$$u(5, x_2) = -x_2^3 + 15x_2^2 + 75x_2 - 125, \ 0 < x_2 < 10.$$

The analytical solution of this problem is

$$u(x_1, x_2) = -x_1^3 - x_2^3 + 3x_1^2 x_2 + 3x_1 x_2^2.$$

The distribution of nodes in numerical example here is the same as that in Fig. 2. And the numerical results from the CVMLPG, together with the exact solution are shown in Figs. 7 and 8. It is again evident that the present results are in excellent agreement with the analytical solutions.

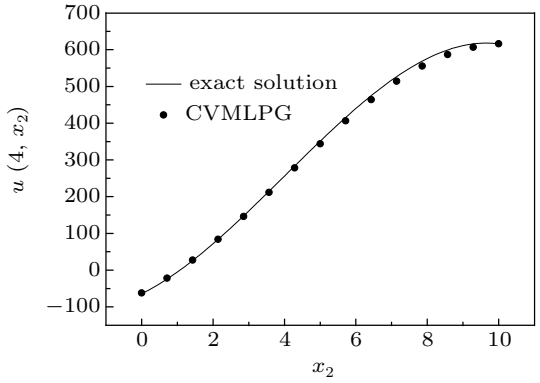


Fig. 7. Exact and numerical solutions of u at $x_1 = 4$.

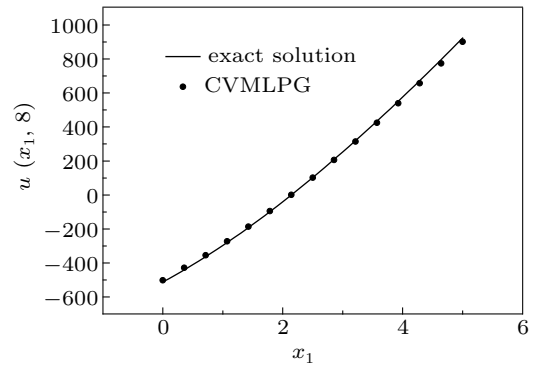


Fig. 8. Exact and numerical solutions of u at $x_2 = 8$.

5. Conclusion

The CVMLPG approach to solving two-dimensional potential problems, based on a local symmetric weak form and the CVMLS, is developed and numerically implemented in the present work. The present method possesses the following advantages over the conventional MLPG.

(i) The trial function of a 2D problem is formed with a 1D basis function.

(ii) The number of unknown coefficients in the trial function of the CVMLS approximation is less than that in the trial function of the MLS approximation.

The numerical results show that fewer nodes are needed in the meshless method that is formed from the CVMLS approximation than those from the MLS approximation. A comparison between the results obtained from the CVMLPG method and the corresponding analytical solutions demonstrates that the

method is both feasible and effective. In essence, the present method possesses a tremendous potential for solving linear and nonlinear boundary value problems, especially for treating those problems with discontinuities and moving boundaries.

References

[1] Minkowycz W J, Sparrow E M, Schneider G E and Pletcher R H 1988 *Handbook of Numerical Heat Transfer* (New York: John Wiley and Sons, Inc.)

[2] Belytschko T, Krongauz Y, Organ D, Fleming M and Krysl P 1996 *Comput. Methods Appl. Mech. Eng.* **139** 3

[3] Zhang X, Liu Y and Ma S 2009 *Adv. Mech.* **39** 1 (in Chinese)

[4] Belytschko T, Lu Y Y and Gu L 1994 *Int. J. Numer. Methods Eng.* **37** 229

[5] Cheng R J and Cheng Y M 2008 *Acta. Phys. Sin.* **57** 6037 (in Chinese)

[6] Atluri S N and Zhu T L 1998 *Comput. Mech.* **22** 117

[7] Zheng B J and Dai B D 2010 *Acta Phys. Sin.* **59** 5182 (in Chinese)

[8] Zheng B J and Dai B D 2011 *Appl. Math. Comput.* **218** 563

[9] Liu W K, Jun S and Zhang Y 1995 *Int. J. Numer. Methods Fluids* **20** 1081

[10] Chen L and Cheng Y M 2010 *Chin. Phys.* B **19** 090204

[11] Cheng Y M and Li J H 2005 *Acta Phys. Sin.* **54** 4463 (in Chinese)

[12] Liew K M and Cheng Y M 2009 *Comput. Methods Appl. Mech. Eng.* **198** 3925

[13] Lancaster P and Salkauskas K 1981 *Math. Comput.* **37** 141

[14] Lu Y Y, Belytschko T and Gu L 1994 *Comput. Methods Appl. Mech. Eng.* **113** 397

[15] Cheng Y M and Chen M J 2003 *Acta Mech. Sin.* **35** 181 (in Chinese)

[16] Liew K M, Feng C, Cheng Y and Kitipornchai S 2007 *Int. J. Numer. Methods Eng.* **70** 46

[17] Cheng Y M, Peng M J and Li J H 2005 *Chin. J. Theor. Appl. Mech.* **37** 1 (in Chinese)

[18] Peng M J, Liu P and Cheng Y M 2009 *Int. J. Appl. Mech.* **1** 367

[19] Bai F N, Li D M, Wang J F and Cheng Y M 2012 *Chin. Phys.* B **21** 020204

[20] Cheng Y M and Li J H 2006 *Sci. Chin.* G: *Phys. Mech. Astron.* **49** 46

[21] Li D M, Peng M J and Cheng Y M 2011 *Sci. Chin.: Phys. Mech. Astron.* **41** 1003 (in Chinese)

[22] Chen L and Cheng Y M 2008 *Acta Phys. Sin.* **57** 1 (in Chinese)

[23] Chen L and Cheng Y M 2008 *Acta Phys. Sin.* **57** 6047 (in Chinese)

[24] Gao H F and Cheng Y M 2009 *Chin. J. Theor. Appl. Mech.* **41** 480 (in Chinese)

[25] Gao H F and Cheng Y M 2010 *Int. J. Comput. Methods* **7** 55

[26] Yang X L, Dai B D and Li Z F 2012 *Acta Phys. Sin.* **61** 050204 (in Chinese)